J. Membrane Biol. 189, 55–66 (2002)
DOI: 10.1007/s00232-002-1004-x

The Journal of
Membrane
Biology



# Single Ionic Channels of Two *Caenorhabditis elegans* Chemosensory Neurons in Native Membrane

**W.T. Nickell, R.Y.K. Pun[1], C.I. Bargmann[2], S.J. Kleene**
Department of Cell Biology, Neurobiology, and Anatomy, University of Cincinnati College of Medicine, P.O. Box 670667 Cincinnati, OH 45267, USA
[1]Department of Molecular and Celluar Physiology, University of Cincinnati College of Medicine, P.O. Box 670576 Cincinnati, OH 45267, USA
[2]Howard Hughes Medical Institute and Programs in Developmental Biology, Neuroscience, and Genetics, Department of Anatomy, The University of California, San Francisco, CA 94143-0452, USA

Received: 28 January 2002/Revised: 20 May 2002

**Abstract.** The genome of *Caenorhabditis elegans* contains representatives of the channel families found in both vertebrate and invertebrate nervous systems. However, it lacks the ubiquitous Hodgkin-Huxley $Na^+$ channel that is integral to long-distance signaling in other animals. Nematode neurons are presumed to communicate by electrotonic conduction and graded depolarizations. This fundamental difference in operating principle may require different channel populations to regulate transmission and transmitter release.

We have sampled ionic channels from the somata of two chemosensory neurons (AWA and AWC) of *C. elegans*. A $Ca^{2+}$-activated, outwardly rectifying channel has a conductance of 67 pS and a reversal potential indicating selectivity for $K^+$. An inwardly rectifying channel is active at potentials more negative than −50 mV. The inward channel is notably flickery even in the absence of divalent cations; this prevented determination of its conductance and reversal potential. Both of these channels were inactive over a range of membrane potentials near the likely cell resting potential; this would account for the region of very high membrane resistance observed in whole-cell recordings. A very-large-conductance (>100 pS), inwardly rectifying channel may account for channel-like fluctuations seen in whole-cell recordings.

**Key words:** Olfaction — Receptor neuron — Electrophysiology — *Caenorhabditis elegans* — Nematode

*Correspondence to:* S.J. Kleene; email: steve@syrano.acb.uc.edu

## Introduction

The nervous system of *C. elegans* uses familiar ionic channels. The genome contains sequences representing all of the known families of $K^+$ channels, voltage-gated $Ca^{2+}$ channels, cyclic-nucleotide-gated cationic channels, and $Cl^-$ channels (Wei, Jegla & Salkoff, 1996; Bargmann, 1998). There is one fundamental omission, however. The Hodgkin-Huxley voltage-gated $Na^+$ channel is basic to signal transmission, coding, and processing in most nervous systems; the varied ionic channels familiar to neurophysiology largely serve to regulate the firing of $Na^+$ action potentials. The Hodgkin-Huxley channel is omitted from the *C. elegans* genome, and electrophysiological recordings find no evidence of fast $Na^+$ currents. In nematode nervous systems, graded depolarization and electrotonic conduction appear to serve functions handled by spikes in other animals. Presumably, the ionic channels of *C. elegans* are adapted to this unique mode of operation.

The only comprehensive electrophysiological studies of nematode neurophysiology are from the parasitic nematode *Ascaris suum*. The resting potential of *Ascaris* neurons and muscle cells is low (−40 mV; del Castillo & Morales, 1967; Brading & Caldwell, 1971; Davis & Stretton, 1989a). Muscle resting potential is nearly independent of $K^+$, but is dependent on $Cl^-$ and organic acids; a large-conductance channel that passes both $Cl^-$ and carboxylic acids may determine the resting potential (Brading & Caldwell, 1971; Robertson & Martin, 1996). The ionic dependence of the membrane potential of *Ascaris* neurons has not been determined. The whole-cell resistance of *Ascaris* neurons is very high; this allows

communication along the length of the neuron by electrotonic conduction (Davis & Stretton, 1989a). Transmitter release is graded around the low resting membrane potential (Davis & Stretton, 1989a). Motor neurons support $Ca^{2+}$-mediated active currents (Davis & Stretton, 1989b).

Because of the difficulty of access and the small size of the neurons, electrophysiological studies of *C. elegans* have been slow to appear. Lockery and coworkers (Goodman et al., 1998; Lockery & Goodman, 1998) described whole-cell recordings from ASER and other neurons in the nerve ring. They found low resting potentials, low resting conductance in the vicinity of the resting potential, and $Ca^{2+}$-mediated active potentials. Richmond and Jorgensen (1999) recorded cholinergic agonist-generated synaptic currents in muscle, but did not report membrane resting potential or membrane resistance.

We are interested in understanding transduction mechanisms in two chemosensory neurons, AWA and AWC. In both of these neurons, odorant specificity and likely second-messenger pathways have been identified by genetic methods (Komatsu et al., 1996; Sengupta, Chou & Bargmann, 1996; Colbert, Smith & Bargmann, 1997; Troemel, Kimmel & Bargmann, 1997; Bargmann & Kaplan, 1998). However, there are substantial neurophysiological differences between *C. elegans* and organisms that are well characterized electrically. Thus, preliminary studies of basic *C. elegans* neural function are necessary before transduction mechanisms can be fully understood. Characterizing the ionic channels present in these neurons would be a good start.

Of the numerous ionic channels represented in the genome, several have already been localized to the membranes of neurons AWA and AWC. A cyclic nucleotide-gated cationic channel (TAX-2/TAX-4) is located primarily in the dendrite of AWC, although channels are also present in the soma (Coburn & Bargmann, 1996; Komatsu et al., 1996). In a heterologous expression system, this channel has a conductance of 56 pS and is best gated by cyclic GMP (Komatsu et al., 1999). OSM-9, a member of the TRPV family of channels, is present in both AWA and AWC, although it serves different functions in the two neurons (Colbert et al., 1997). The electrophysiological properties of this channel have not been reported. SLO-1 and SLO-2 BK $K^+$ channels are present in numerous unidentified neurons of the nerve ring. When expressed in frog oocytes, these channels have large conductances; some are activated by $Ca^{2+}$ and/or $Cl^-$ (Yuan et al., 2000).

Heterologous expression provides a powerful means of determining the properties of genetically identified channels but cannot tell us how those channels function in their native environment. In the neuron, gene products may be altered before insertion into the membrane, combined with other subunits in unknown proportions, or regulated by internal messengers. Tissue culture of embryonic cells provides a closer approximation to in vivo conditions (Christensen et al., 2002). Embryonic neurons express important markers and exhibit currents similar to those observed in adult neurons. However, cultured neurons lack normal cell-cell interactions and morphological specializations. For these reasons, functional properties of the channels must be determined in the native membrane. We have chosen to record from identified chemosensory neurons AWA and AWC in adult worms. Cell-attached recording from these neurons is as close as we can come to an in vivo recording; it is likely that the soma and dendritic ending remain intact. In our preliminary survey, single channels appear to fall into a small number of classes. While it is presently impossible to match these channels with reported genes, more detailed studies of channel properties and continued progress in genetic analysis should make this an attainable goal. The properties of the common channels appear to account for the whole-cell properties of *C. elegans* neurons observed by ourselves and others. Less common large-conductance channels may also play important roles in neuronal function.

## Materials and Methods

### Exposure of Neurons (Overview)

The somata of the 24 amphid chemosensory neurons are located in the anterior sensory ganglion, just rostral to the terminal bulb of the pharynx. Processes of these neurons extend anteriorly to join in the circumpharyngeal nerve ring (Ward et al., 1975; Ware et al., 1975). Each chemosensory neuron also extends one dendrite anteriorly to one of the two amphid sensilla, where it is exposed to the environment (Fig. 1*A*). We used strains of worms in which either the AWA (kyIs 37 (*odr-10::*GFP)) or AWC (kyIs 136 (*str-2::*GFP)) neurons express green fluorescent protein (GFP; Chalfie et al., 1994). Both the dendrites and axons of the labeled neurons are clearly visible under fluorescence microscopy (Fig. *1A*).

To expose GFP-labeled AWA or AWC neurons, we cut the worm at about the level of the terminal bulb (near the dashed lines in Fig. 1, *A* and *B*). Contraction of body-wall muscles in the "head" then exposed the terminal bulb and some of the neurons (Fig. 1, *C* and *D*; Avery, Raizen & Lockery, 1995). In 5–10% of the cut worms, at least one GFP-labeled neuron was intact and exposed. Successful recordings required preparation of many worms to ensure an adequate number of accessible neurons.

Worms maintain a high turgor pressure; cutting them under standard saline (Dent's Solution; Avery et al., 1995) results in explosive release of worm contents. GFP-labeled neurons exposed after this treatment often appeared swollen and typically disappeared within one hour after cutting. The internal pressure is probably due to a combination of osmotic pressure and tonic muscle contraction (Hobson, Stephenson & Beadle, 1952a; Hobson, Stephenson & Eden, 1952b; Harris & Crofton, 1957; Pax et al., 1995). To minimize damage to neurons, internal pressure was reduced by equilibrating worms in a low-tonicity medium before cutting them in a physiological saline containing an additional 100

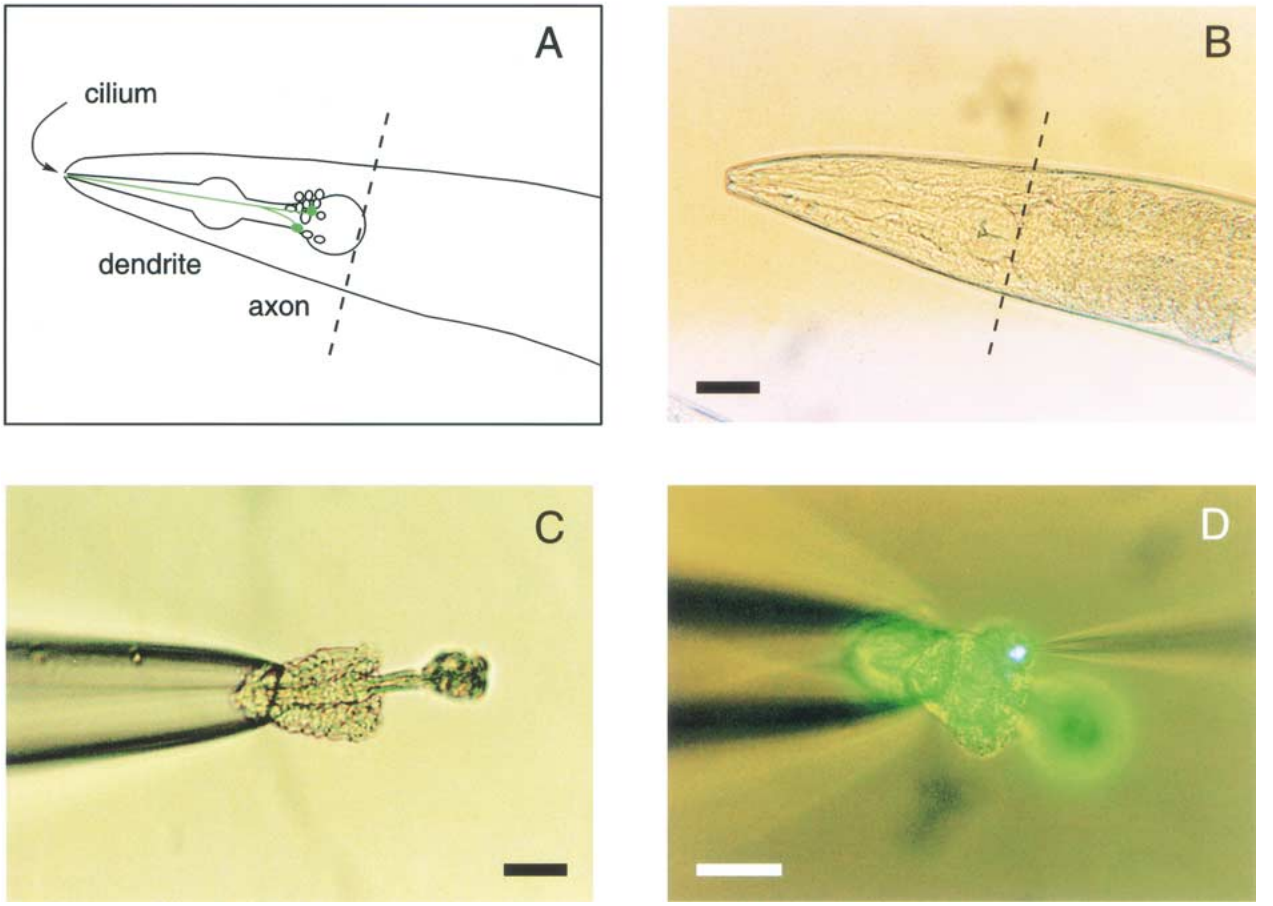


**Fig. 1.** Recording method. (*A,B*) Structure of worm (modified from Sengupta et al., 1996). Neurons are located anterior to the terminal bulb of the pharynx. On each side of the animal, 12 chemosensory neurons each send a single dendrite to the ipsilateral amphid sensillum in the "nose". To expose the neurons, a cut is made at about the level of the dashed line. The neurons AWA and AWC are indicated in green. (*C*) Worm head in a suction pipette. After the cut, contraction of body-wall muscles pulls the nerve ring away from the pharynx. The suction pipette may also grasp the head from the side or the terminal bulb, allowing application of odorants. (*D*) Combined fluorescence and phase-contrast image of a worm head. A recording pipette approaches a fluorescent neuron. Calibration bars: 25 μm.

mM sucrose or 50 mM Na acetate (Sucrose or Acetate Dent's Solution; *see* Table 1). This saline also contained 200 μM of the cholinergic agonist carbachol, which may have improved exposure of the neurons by increasing contraction of body-wall muscles (Avery et al., 1995). More importantly, carbachol blocked spontaneous movements of the severed head, which otherwise continued indefinitely in Dent's Solution.

## Exposure of Neurons (Detailed Procedure)

Under a dissecting microscope, approximately 100 adult worms were transferred from culture plates to a dish containing 0.5% NaCl. Worms were left in this solution for 10–30 min to allow equilibration to a relatively low osmotic pressure. Worms were then transferred to a pool of Sucrose or Acetate Dent's Solution (*see* Table 1) confined by a ring of silicone grease to a plastic sheet (Mylar drawing film or overhead projector transparency) glued to an anodized aluminum heat sink. The cooling fins of the heat sink were partially immersed in ice water; this immobilized the worms. Worms were cut with a hand-held #11 scalpel blade under 40× magnification. The severed heads, roughly 50 μm in length after contraction of the body-wall muscle, were transferred individually to a recording chamber using a suction pipette.

To allow inspection of many worm heads, heads were initially placed in a large (15 × 20 × 1 mm) pool. As perfusion of this pool would expose the entire population of heads to altered ionic environments, recordings were performed in a second, smaller pool (1 cm in diameter) which was continuously perfused at a rate of 0.2 ml/min. A 3-mm-wide saline-filled path connected the two pools, allowing the heads to remain submerged while being moved between the pools. The chamber was cut from 1-mm-thick refrigerator magnet stock using a standard-thickness coverslip as the bottom.

## Recording

The chamber was placed on an inverted microscope (Nikon Diaphot equipped with a 100-W mercury burner for epi-illumination and a Chroma Technologies Longpass Endow filter set with excitation peak at 470 nm and an emission filter cutoff of 500 nm). A selected head was captured in a suction pipette (Fig. 1*C*). Actual contact of the neuron by the recording pipette was monitored using a 40× water-immersion phase-contrast objective (0.75 NA; Fig.

**Table 1.** Solutions

| ITEM | Sucrose Dent's | Acetate Dent's | Internal Solution | Excised Patch Pipette Solution | Perforated Patch Pipette Solution | Calcium-Test Pipette Solution | Calcium-Test Hi-Ca Cytoplasmic Solution | Calcium-Test Lo-Ca Cytoplasmic Solution |
|---|---|---|---|---|---|---|---|---|
| NaCl | 140 | 140 | 5 | 140 | 10 | 140 | 0 | 0 |
| K Acetate | 0 | 0 | 0 | 0 | 0 | 0 | 0 | 0 |
| Na Acetate | 0 | 50 | 0 | 0 | 0 | 0 | 0 | 0 |
| KCl | 6 | 6 | 141.5 | 5 | 70 | 0 | 40 | 40 |
| $K_2SO_4$ | 0 | 0 | 0 | 0 | 30 | 0 | 0 | 0 |
| $CaCl_2$ | 3 | 3 | 1 | 0 | 0 | 0 | 0 | 0 |
| $MgCl_2{\cdot}6H_2O$ | 1 | 1 | 0 | 0 | 0 | 1 | 0 | 0 |
| K HEPES | 0 | 0 | 10 | 0 | 10 | 0 | 10 | 10 |
| Na HEPES | 5 | 5 | 0 | 10 | 0 | 10 | 0 | 0 |
| EGTA | 0 | 0 | 5 | 5 | 0.5 | 0 | 0 | 5 |
| Glucose | 10 | 10 | 0 | 0 | 0 | 0 | 0 | 0 |
| Sucrose | 100 | 0 | 100 | 100 | 100 | 0 | 0 | 0 |
| Na Gluconate | 0 | 0 | 0 | 0 | 0 | 70 | 0 | 0 |
| K Gluconate | 0 | 0 | 0 | 0 | 0 | 0 | 175 | 165 |
| hemiCa Gluconate | 0 | 0 | 0 | 0 | 0 | 0 | 0.2 | 0 |

1*D*). Both the fluorescent neuron and the recording pipette were visible with the combination of phase-contrast and epifluorescence.

The bath was not perfused during cell-attached recordings. For perforated-patch intracellular recordings, the pipette was filled with standard intracellular saline adjusted to the higher osmolarity of the extracellular solution (*see* Table 1, Perforated-Patch Pipette Solution). Pipette tips were filled with this solution before backfilling the pipette with saline containing 250 μg/ml nystatin or gramicidin.

For inside-out excised-patch recordings, the selected head was transferred to the smaller pool of the chamber (remaining under saline throughout), and the saline-filled path between the two pools was blocked with a plug of silicone wax. Seals were formed in Dent's Solution using a recording pipette filled with high-$Na^+$/0 $Ca^{2+}$ solution (Excised-Patch Pipette Solution). Immediately after seal formation, the perfusing solution was switched to Internal Solution. After 2 min, the recording pipette was withdrawn 10 μm to excise the patch. Solution compositions are given in Table 1.

Recording pipettes were pulled on a computer-controlled puller from thin-walled borosilicate tubing (Corning 7740) or standard-wall low-melting-temperature borosilicate tubing (type 8250; Garner Glass Company, Claremont, CA). Optimal electrode resistance for the thin-walled tubing was about 8 MΩ; somewhat higher resistances (10–15 MΩ) were optimal for the standard-wall glass. Pipettes were usually coated with silastic (Dow-Corning Sylgard 184) to reduce capacitance artifacts. Suction pipettes for capturing worm heads were pulled from soda-lime glass hematocrit tubes in two stages on a Brown and Flaming type puller (Sutter Instrument Company). Optimal suction pipettes had a very long shank (1 cm) and a fire-polished tip diameter of about 35 μm. The long shank made the pipette flexible enough that it did not break on gentle contact with the chamber bottom. In addition, the long pipette shank created sufficient flow resistance to prevent unavoidable small pressures in the pipette from creating significant fluid flow, which scattered worm heads and prevented their capture.

Currents were recorded using an Axopatch 1D or Axopatch 200B patch-clamp amplifier. Current signals were filtered at 2 kHz using the internal filter of the instruments and were digitized at 5 kHz using a Digidata 1200B data-acquisition board and an IBM-compatible computer. Command signal generation and data acquisition were controlled using pCLAMP software from Axon Instruments. The Axon Instruments program Axograph was used for data analysis and display. For perforated-patch whole-cell recordings, leak currents have been subtracted using the standard routines of the pCLAMP software (p/8 protocol); the raw signals (not leak-subtracted) were recorded on a separate channel. Except where noted, leak currents were subtracted from the single-channel records reproduced here. The holding potential was routinely set at −35 mV. *I-V* relations of single channels were determined by manually measuring the amplitude of at least 4 well-defined channel openings using the Axograph software.

Figs. 3, 5, 6, and 7 display amplitude histograms for single-channel recordings as probability density functions (PDFs). Each number in parentheses on these figures represents the fraction of the total area of a Gaussian function fitted to the peak.

## Solutions

Because of the small size of *C. elegans*, the composition of its internal environment has not been determined. The obvious model solution for *C. elegans* is normal *Ascaris* saline, which has a relatively high osmolarity (323 mOsm), high $K^+$, and low $Cl^-$; the missing $Cl^-$ is replaced by $acetate^-$, which simulates a high concentration of long-chain carboxylic acids produced by anaerobic muscle metabolism. *Ascaris* saline, however, does not support normal pharyngeal pumping in *C. elegans* (Avery et al., 1995). Pharyngeal activity *does* continue in solutions containing lower $K^+$, $Cl^-$, and no $acetate^-$ (Dent's solution, 285 mOsm; Avery et al., 1995). Later work by Lockery and Goodman used solutions of higher osmolarity (315–325 mOsm), which were believed to preserve neuronal health (Lockery and Goodman, 1998). Richmond and Jorgensen (1999), in their recordings from *C. elegans* muscle, used a solution more similar to *Ascaris* saline. In the present work, the ionic composition of the solutions was essentially identical to the solutions found appropriate by Avery et al. (1995; Dent's solution) except that osmolarity was increased for reasons explained above. In initial work, osmolarity was increased by addition of 100 mM sucrose. Later experiments used 50 mM Na acetate instead of the sucrose, in an effort to make the solution more similar to *Ascaris* saline. We retained the high-osmolarity solution throughout the recording periods because neurons appeared healthy in the

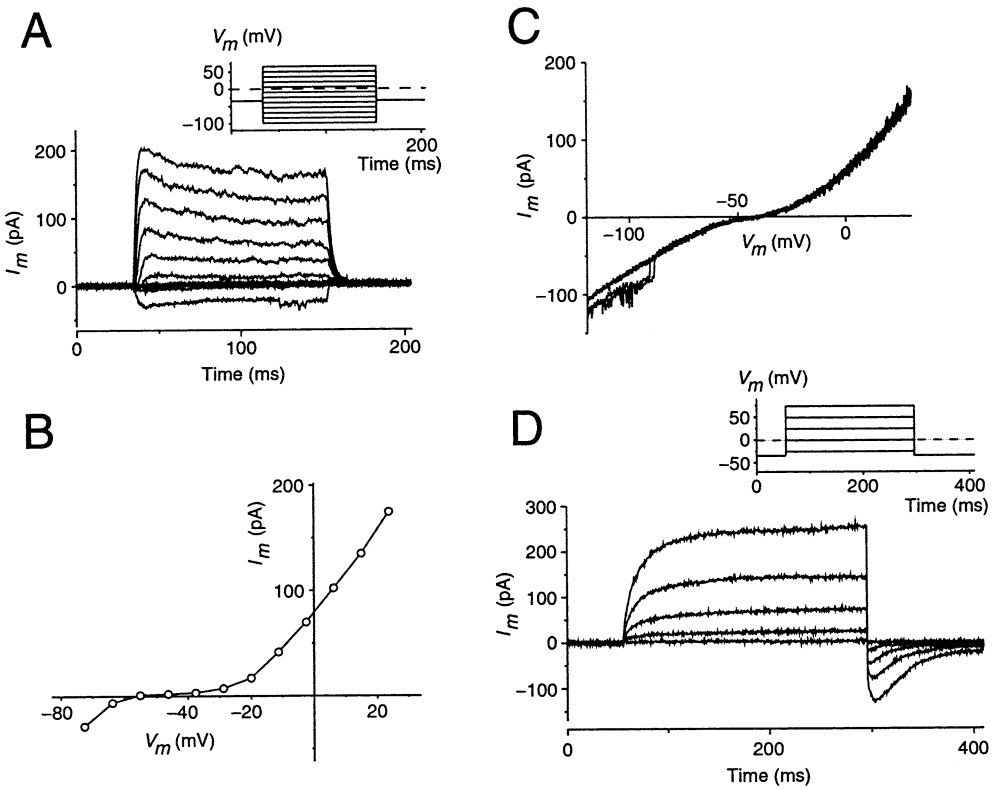


**Fig. 2.** Whole-cell perforated-patch currents. (*A*) Whole-cell currents. Note the apparent single-channel activity on the bottom trace (AWA neuron with gramicidin perforation, leak-subtracted). (*B*) *I-V* relation derived from the cell in *A* without leak subtraction. (*C*) Voltage ramp, −120 mV to +30 mV. Four sweeps are superimposed. Note the single-channel openings on two of the four sweeps (AWA neuron with nystatin perforation). (*D*) Tail currents (AWC neuron with nystatin perforation).

solution, and because replacing it with a low-osmolarity solution would have complicated the procedures.

The measured tonicity of our physiological solution was 380 mOsm, and the pH was adjusted to 7.4. In this solution, severed heads maintained spontaneous movement and occasional pharyngeal pumping for several hours. GFP-labeled neurons also maintained a normal appearance and brightness for hours. The osmotic strength of internal and pipette solutions was adjusted to match the physiological saline. The compositions of all solutions used are summarized in Table 1.

## Results

### Perforated-Patch Whole-Cell Recording

Perforation was judged to be successful if the resting potential was more negative than −15 mV and inward currents were seen on depolarization. Successful recordings were obtained from more than 50 somata. In the majority of these neurons, the resting potential was low and the only active current was a slowly activating outward rectifier. Fig. 2*A* illustrates representative records from an AWA neuron that appeared intact. Records are leak-subtracted. Depolarization to potentials more positive than −20 mV produced a substantial outward current. A part of this current inactivated. An inward current was activated at potentials more negative than −70 mV. Fig. 2*B* shows the current-voltage (*I-V*) relation derived from the same recordings as in Fig. 2*A*, but without leak subtraction.

Figure 2*C* shows the *I-V* relation measured directly in a different AWA neuron during voltage ramps between −120 and +30 mV membrane potential. Four sweeps are superposed. In this cell, the zero-current potential was −40 mV; the region of high resistance extended from −40 mV to −60 mV. In two of the trials, an apparent large-conductance single channel opened during hyperpolarization.

An inward tail current recorded from an AWC neuron is illustrated in Fig. 2*D*. These records were obtained from an incomplete cell lacking a dendrite and axon. Smaller, but similar tail currents were observed in 3 intact neurons. The decay constants for the two largest tail currents (single-exponential fit using the Axograph software) were 26.8 and 17.9 msec. Fig. 2*D* also illustrates a slowly activating outward current.

The true resting potential of *C. elegans* neurons is an important parameter that has not yet been determined with any certainty. In a sample of 21 consec-

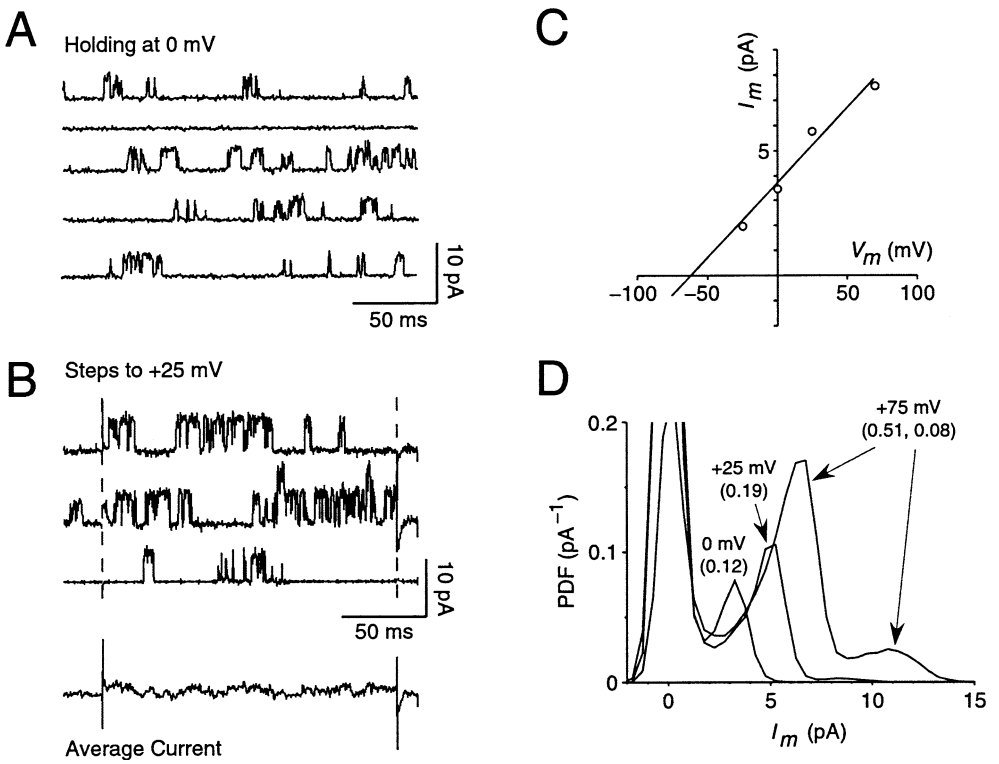


**Fig. 3.** Outwardly rectifying channels in excised patches. The pipette was filled with Excised-patch Pipette Solution; the bath contained Internal Solution, which is low in $Ca^{2+}$ (Table 1). (*A*) Representative recordings while holding at 0 mV. (*B*) Representative recordings during steps from 0 mV to +25 mV. The bottom trace in *B* is the average of 20 traces. No inactivation is apparent. (*C*) *I-V* relation derived from the same patch. Conductance is 60 pS; the reversal potential is −61 mV. The equilibrium potential for $K^+$ was −81 mV. (*D*) Probability density functions (PDFs) determined in the same patch. Each trace is constructed from 20 voltage steps to the indicated membrane potential. During the jump to +75 mV, there were a sufficient number of double channel openings to produce a secondary peak in the PDF.

utive cells in which there was apparent perforation, 17 had zero-current potentials clustered between −16 and −22 mV; 4 had substantially higher potentials (−65, −31, −37, and −44 mV).

## Single Outwardly Rectifying Channels

Figure 3 shows an outwardly rectifying channel recorded in an excised patch with the cytoplasmic face exposed to Internal Solution (Table 1), which is low in $Ca^{2+}$. In this patch, clear single-channel fluctuations were visible at potentials more positive than −25 mV. Open probability increased greatly with increasing depolarization. Selected recordings obtained at 0 mV and +25 mV are illustrated in Fig. 3*A* and *B*. The average of multiple voltage jumps did not reveal any slow activation or inactivation (bottom trace in Fig. 3*B*). In the illustrated channel, current amplitudes were linearly related to membrane potential with a slope conductance of 60 pS and an extrapolated reversal potential of −61 mV (Fig. 3*C*). Channel amplitudes were estimated by manually measuring the amplitude of well-defined channel openings using the Axograph software. For four channels for which an *I-V* relation was obtained, the mean conductance was 53 pS (range 48–60 pS). The mean reversal potential was −60 mV (range −39 to −74 mV). Only $K^+$ had a negative reversal potential in these experiments ($E_K$ = −81 mV). Thus it is likely that this channel conducts $K^+$, although it may be somewhat permeable to other ions as well. Fig. 3*D* shows probability density functions (PDFs) derived from this patch at the three holding potentials indicated. As documented by the fractional areas of the PDF peaks (shown in parentheses), opening probability increased sharply with positive membrane potentials.

A rapidly inactivating outward rectifier is illustrated in Fig. 4. Similar channels were present in two other patches. Although it was not possible to construct an *I-V* relation for these channels, the conductance was small. The average current for the illustrated channels at +100 mV was 0.9 pA. The average of 20 records (lower trace in Fig. 4*A*) inactivates with a decay constant of 21 msec. Fig. 4*B* illustrates currents from a whole-cell recording in which the inactivating outward current was prominent. Decay constants for the current are indicated on the figure.

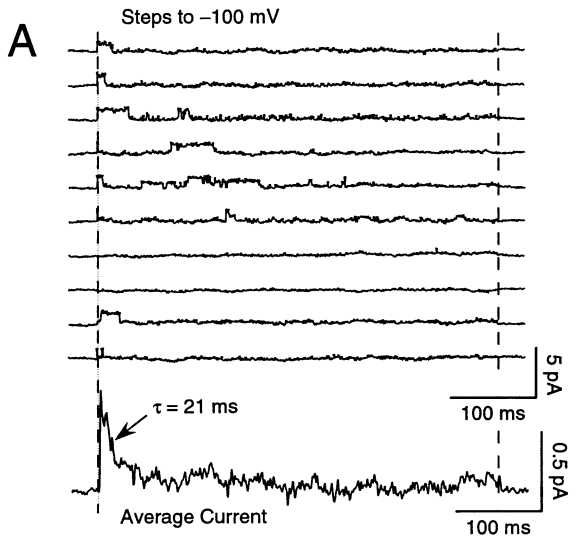


**Fig. 4.** Rapidly inactivating channel. (*A*) Selected traces of depolarizing steps to −100 mv (pipette potential; cell-attached AWA neuron with Sucrose Dent's Solution in the pipette). The bottom trace is the average of 20 traces and shows inactivation. *I-V* relations could not be obtained, but channel conductance is substantially lower than that of the typical outward channel illustrated in Fig. 3. (*B*) Perforated-patch recording showing prominent macroscopic inactivating currents (AWC neuron with nystatin perforation, membrane potential −28 mV).

## $Ca^{2+}$ Activation of Outwardly Rectifying Channels

$Ca^{2+}$-activated $K^+$ channels are present in the *C. elegans* nervous system (Yuan et al., 2000). We conducted a series of experiments to assess whether such channels could be identified in AWA neurons (Fig. 5). Of 16 successful patches, 8 contained outwardly rectifying channels in 100 μM cytoplasmic $Ca^{2+}$. In each patch, channels were absent or only activated at high positive membrane potentials in the absence of $Ca^{2+}$. In 5 of 8 patches, the effect of $Ca^{2+}$ was shown to be reversible. In the remaining cases, the patch was lost before reversal could be accomplished.

Fig. 5 illustrates the characteristics of these channels in a typical excised patch. With low levels of $Ca^{2+}$ present, channel openings were frequent during a step to +100 mV. In steps to +50 mV, a small outward channel was present, but the large channel did not open (Fig. 5*A*, top pair of records; Fig. 5*C*). Addition of 100 μM $Ca^{2+}$ allowed the channel to gate at less positive potentials. Channel openings were present at 0 mV and more positive potentials (Fig. 5*A*, middle pair of records; Fig. 5*D*). Removing $Ca^{2+}$ from the bath reversed this effect (Fig. 5*A*, bottom pair of records).

The *I-V* relations of these channels are summarized in Fig. 5*B*. In these trials, the pipette contained Calcium-test Pipette Solution; the cytoplasmic face of the patch was exposed to Calcium-test Hi-Calcium Solution or Calcium-test Low-Calcium Solution. To obtain data over the entire voltage range, channel openings from both the high- and low-$Ca^{2+}$ conditions were plotted together. The regression line indicates a conductance of 67 pS and a reversal potential of −50 mV.

## Inward Flickering Channels

In a sample of 20 successive excised patches from AWC neurons, 11 exhibited similar flickery inward channels when the membrane was polarized more negative than −100 mV. A similar proportion of patches from AWA neurons contained such currents. Characteristics of the most common inward rectifier are illustrated in Fig. 6. Current fluctuations were visible at −50 mV. The channel showed greater activity on hyperpolarization to −70 mV (Fig. 6*A*) and more negative potentials. Discrete channel openings were not apparent. No peaks could be identified in the probability density functions at −75 and −50 mV (Fig. 6*B*). However, in many patches the periods of activity showed distinct onsets and offsets, suggesting single-channel activity (Fig. 6*A*). Some voltage steps produced no openings, while others resulted in bursts of activity or a prolonged opening. We have not precisely determined the reversal potential of this channel. However, the presence of inward currents at −50 mV indicates that the reversal potential is more positive than this. Under the ionic conditions of these experiments, $Cl^-$ and $Na^+$ had reversal potentials more positive than −50 mV. Hence, the inwardly rectifying channels may be permeable to either of these ions or may be nonselective cationic channels.

The inwardly rectifying channel appeared to be slowly activating at negative potentials. At 0 mV, the

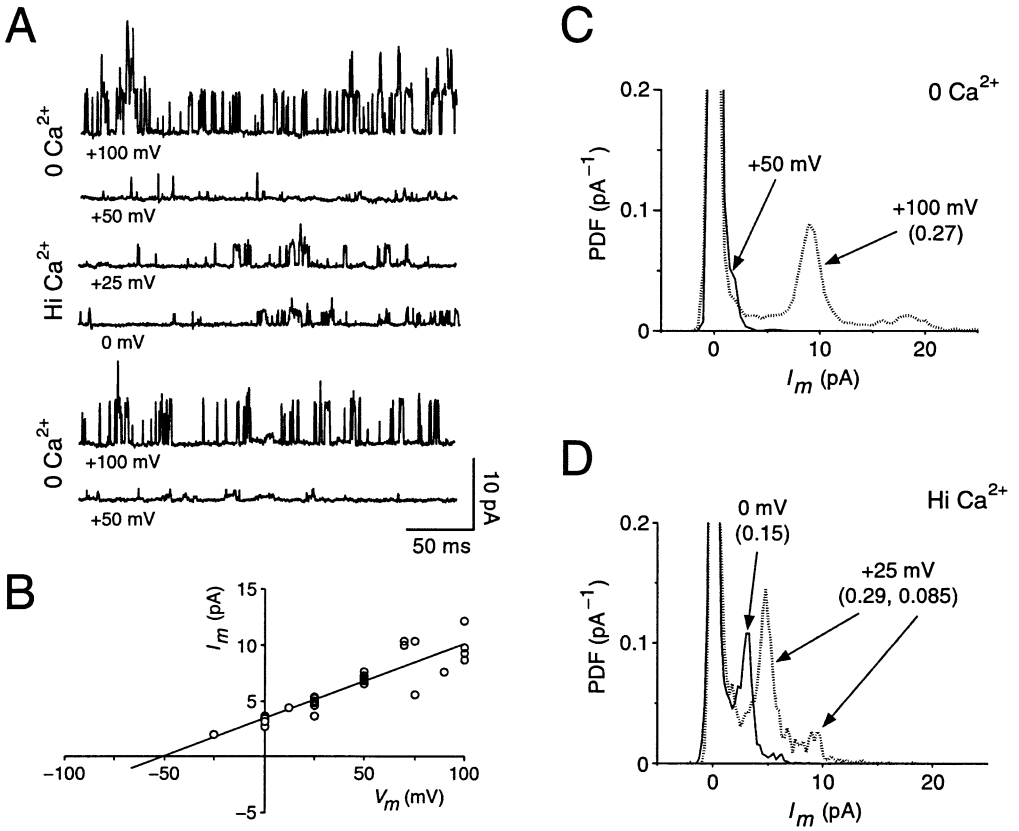


**Fig. 5.** $Ca^{2+}$-activated channels in excised patches. In all cases, the pipettes contained Calcium-Test Pipette Solution. (*A*) Portions of 250-msec steps to the indicated potentials. Top two traces: Steps to +50 and +100 mV in Calcium-Test Lo-Ca cytoplasmic solution. Channel openings were frequent at +100 mV but not at +50 mV. A small-conductance channel was also present in this patch; openings were visible at +50 mV. Middle two traces: In Calcium-Test Hi-Ca cytoplasmic solution (100 μM $Ca^{2+}$), channel openings were frequent at 0 mV and +25 mV and more positive potentials. Above +50 mV, multiple channel openings were observed (*not shown*). Lower two traces: Return to the Lo-Ca solution reversed the effect of increased $Ca^{2+}$. (*B*) *I-V* relation using data pooled from 8 patches. The conductance, estimated from linear regression through all points, is 67 pS, with a reversal potential of −50 mV. (*C,D*) PDF functions derived from the patch illustrated in (*A*).

recordings were stable. At −70 mV, channel activity consistently increased for several minutes following seal formation. This slow activation was apparent in 200-msec steps to −70 mV (Fig. 6*A*). Fig. 6*C*, which is the average of 20 voltage steps, shows an increase in current toward the end of the recording.

## Large-Conductance Inward Channels

We also observed large-conductance, inwardly rectifying channels. These are evidently rare or are rapidly inactivated following excision of the patch. In more than 100 cell-attached and excised patches, only 11 of these channels were seen. Four were observed while cell-attached; these disappeared after excision of the patch into a low-$Ca^{2+}$ solution. The remaining 7 were observed in excised patches. For two of these, the pipette contained Excised Patch Pipette Solution, while low-$Ca^{2+}$ Internal Solution bathed the cytoplasmic face of the patch. Four were observed with Calcium-test Hi-Ca solution bathing the cytoplasmic face and Calcium-test Pipette Solution in the pipette. One was observed only with Dent's solution, a high-$Ca^{2+}$ solution, bathing both sides of the membrane. In excised patches, the channel was seen only transiently. Seven of these channels were recorded from AWA neurons; the remaining 4 were recorded from AWC neurons.

The properties of an inward channel observed in cell-attached mode are illustrated in Fig. 7*A* and *B*. The apparent conductance of this channel was 120 pS. Current reversed when the pipette was held at −10 mV. If the cell resting potential was −20 mV, the actual reversal potential of the channel would be −10 mV membrane potential. The observed conductance of this channel could have been reduced by the high membrane resistance of the intact cell membrane, which would appear as a resistance in series with the channel conductance. The channel was activated by hyperpolarization (Fig. 7*B*).

Fig. 7*C* illustrates the *I-V* relation from 3 excised patches using the Calcium-test solutions. In these

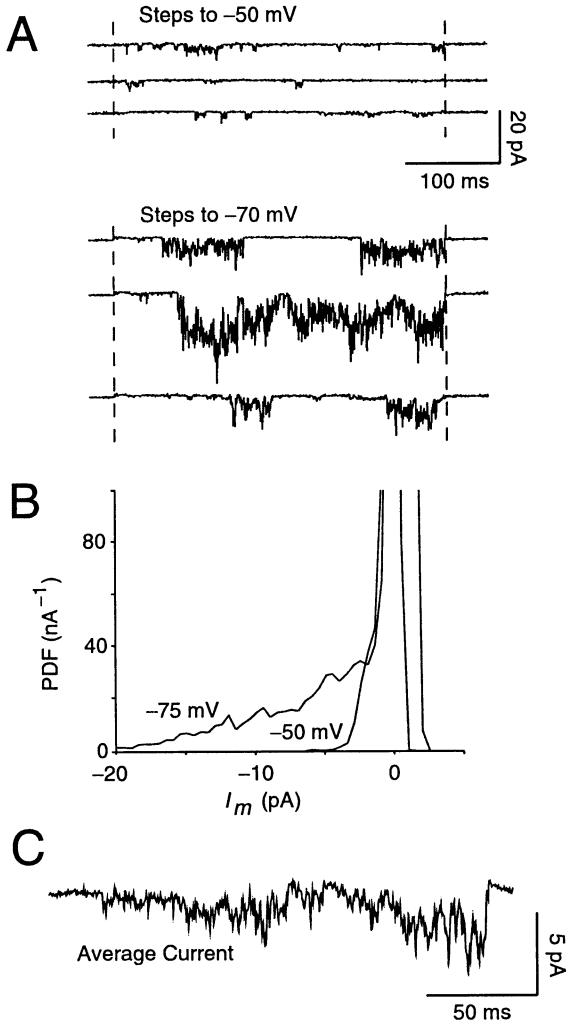


**Fig. 6.** Hyperpolarization-activated inward currents. (*A*) Inward currents are visible at potentials more negative than −50 mV and are flickery even in the absence of divalent cations (excised patches from AWC neurons). The pipette contained Excised-Patch Pipette Solution; the bath contained Internal Solution (Table 1). The abrupt onset and stopping of current events suggest channel activity. (*B*) Probability density functions (PDFs) derived from the patch in *A*. No peak amplitude is detectable. (*C*) Average of 20 successive jumps to −70 mV. The activity of the channel increases with time.

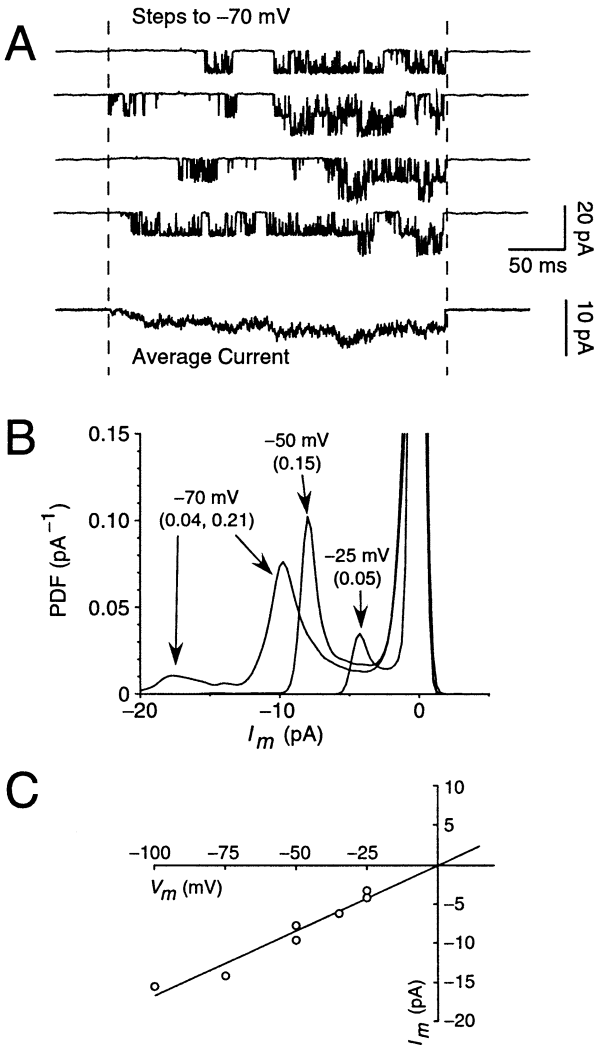


**Fig. 7.** Large-Conductance Inward Channels. (*A*) *Top four traces*: Representative recordings while cell-attached. The pipette contained Calcium-Test Pipette Solution. Channel conductance was 120 pS and reversed when the pipette potential was −10 mV. *Lower trace*: Average of 20 voltage jumps to −70 mV. (*B*) Probability density functions (PDFs) of the channel shown in *A* at the indicated potentials. Multiple channel openings at −70 mV produced a secondary peak. (*C*) *I-V* relation derived from 3 excised patches. The pipette contained Calcium-Test Pipette Solution; the cytoplasmic face was exposed to Calcium-Test Hi-Ca or Calcium-Test Lo-Ca cytoplasmic solution. The channel conductance was 166 pS; the reversal potential was +1 mV.

solutions, the reversal potentials for $Na^+$ and $K^+$ were very positive and very negative, respectively. $Cl^-$ was also asymmetrically distributed, with a reversal potential of −32 mV. The *I-V* relation reverses at +1 mV, suggesting that the channel is a nonselective cation channel.

Reliable *I-V* relations were obtained for 9 such channels in cell-attached or excised-patch recordings. In each case the channel conductance was greater than 100 pS (mean 163 pS; range 108–255). Reversal potentials ranged from −16 to +4 mV (membrane potential) for the excised patches and from −12 to +2 mV (pipette potential) while cell-attached.

## Discussion

### Whole-cell Properties

On several points, our perforated-patch whole-cell recordings are in agreement with previous recordings from *C. elegans* neurons. The resting potential is low. There is a region of very high membrane resistance between about −20 and −70 mV; this region is bounded by inwardly and outwardly rectifying

currents. There is a notable absence of currents resembling fast action potentials.

There are a few notable differences in technique between previously reported whole-cell recordings and ours. First, we gained access to the cell interior by perforating rather than rupturing the patch; perforation eliminates the dialysis of cytoplasmic components. The similarity of our results to those of Goodman et al. (1998) suggests that washout does not greatly alter these basic currents. Second, we routinely clamped the cell membrane potential at −35 mV rather than the more negative values commonly used for neurons having Hodgkin-Huxley action potentials. We considered this holding potential to be nearer the physiological value because that is the resting potential of *Ascaris* neurons and because many of our excised patches became unstable at membrane potentials more negative than −70 mV. Finally, our recordings were exclusively from adult neurons.

Our whole-cell recordings show that the following currents are present in AWA and AWC: (1) an inwardly rectifying current activated at potentials more negative than −50 mV; (2) an outwardly rectifying current activated at potentials more positive than −20 mV; (3) an inward tail current (Fig. 2*D*) which may be activated by $Ca^{2+}$; (4) an inactivating component of the depolarization-activated outward current; and (5) a slowly activating component of the hyperpolarization-activated inward current.

## Single-Channel Properties

The common inwardly and outwardly rectifying single channels appear to account for the steady-state whole-cell currents. The activation voltages of the single channels coincide well with the activation voltages of the whole-cell currents. Similar channels were present in cell-attached and excised-patch recordings, in both AWA and AWC neurons, and independent of the presence of divalent cations. This suggests that these channels may provide the basic resting currents of *C. elegans* neurons.

## Outwardly Rectifying Channels

We observed outwardly rectifying channels that were activated by depolarization (Figs. 3–5). Some were also activated by $Ca^{2+}$ (Fig. 5); these are somewhat similar to $K^+$ channels of the SLO family as measured after heterologous expression. Both the *slo-1* and *slo-2* genes are expressed in an overlapping pattern in neurons of the nerve ring (Yuan et al., 2000). In isolation, both of these channels are sensitive to $Ca^{2+}$. The open probability of the SLO-2 channel is, in addition, modulated by $Cl^-$. Since the two related channels may be expressed in the same neurons, the channel actually functioning in neurons may be a heteromultimer.

## Inwardly Rectifying Channels

We observed two types of inwardly rectifying channels, both activated by hyperpolarization (Figs. 6,7). The first type (Fig. 6) is flickery and difficult to characterize. The reversal potential could not be measured, but it is more positive than −50 mV. Under the ionic conditions of these experiments, the possible ionic selectivities include: $Na^+$, nonselective cationic, or $Cl^-$. The *C. elegans* genome contains genes for 6 $Cl^-$ channels, 6 cyclic-nucleotide-gated (CNG) channels, and 11 TRP-like channels (Bargmann, 1998). The latter two types are typically nonselective cationic channels. Two CNG channel monomers are present in AWC, although these are primarily located at the end of the dendrite rather than in the soma (Coburn & Bargmann, 1996; Komatsu et al., 1996, 1999). Typically, CNG channels are flickery in the presence of divalent cations, but not in their absence. The present channels were flickery even in divalent-free solutions. A member of the TRPV family of channels (OSM-9) is present in both AWA and AWC (Colbert et al., 1997). Some of the 6 $Cl^-$ channels of *C. elegans* are expressed in neurons and produce inwardly rectifying currents on heterologous expression (Schriever et al., 1999; Nehrke et al., 2000). Their single-channel properties have not yet been described.

The large-conductance inwardly rectifying channel (Fig. 7) is most probably a nonselective cation channel. In all of the excised patches studied, the channel reversed within the range −16 to +4 mV. In some of these experiments, the reversal potential for $Cl^-$ was −32 mV, making it unlikely that $Cl^-$ was the current-carrying ion.

## Normal Neuronal Function

Although there are significant differences between *C. elegans* and *Ascaris*, the striking similarities in anatomy and connectivity suggest that *Ascaris* motorneurons (Davis & Stretton, 1989a,b) provide reasonable hypotheses about the normal operation of the nervous system of *C. elegans*. The −40 mV resting potential of *Ascaris* neurons would sit squarely in the middle of the region of high membrane resistance observed in neurons of *C. elegans*. Very small currents induced in the tip of the dendrite by odorant transduction could then move the potential of the soma between the two limits set by the inward and outward rectifiers. Transmitter release in *Ascaris* is graded as a function of membrane potential (Davis & Stretton, 1989b). Tonic transmitter release would be

determined by the normal resting membrane potential; that potential is therefore of substantial physiological significance.

### Resting Potential

Determination of the resting potential of very small cells is an inherently difficult problem. When the cell membrane resistance is comparable to the patch gigaseal resistance, shunt currents across the seal reduce the observed potential. On the other hand, small offset currents or an electrogenic pump could shift the zero-current potential by tens of millivolts. Because we cannot yet resolve the true membrane and seal conductances, the precise resting potential remains uncertain.

The normal resting potential is further uncertain because neither the ionic basis of the potential nor the proper ionic composition of the bathing solutions has been determined. Relatively small changes in $K^+$ or other permeant ions could alter the resting potential significantly. Further, as illustrated by the relative independence of *Ascaris* muscle membrane potential from $K^+$ (del Castillo & Morales, 1967; Brading & Caldwell, 1971; Robertson & Martin, 1996), it is possible that the resting potential of *C. elegans* neurons is determined by ions other than $K^+$.

## Conclusion

We have conducted a first survey of the channels that underlie whole-cell currents in two *C. elegans* chemosensory neurons. Further study of the modulation and gating properties of these channels should provide insight into the normal function of *C. elegans* neurons. Although the problem is not simple, association of the major ionic channels and currents with genes seems a reasonable objective. Further work is needed to explore the ionic selectivities, voltage sensitivities, pharmacology, and modulation of these currents.

We are grateful to Dr. Shawn Lockery for helpful discussions. This work was supported by research grant number 5 R01 DC 04203 from the National Institute on Deafness and Other Communication Disorders, National Institutes of Health.

## References

Avery, L., Raizen, D., Lockery, S. 1995. Electrophysiological methods. *Meth. Cell Biol.* **48**:251–269

Bargmann, C.I. 1998. Neurobiology of the *Caenorhabditis elegans* genome. *Science* **282**:2028–2033

Bargmann, C.I., Kaplan, J.M. 1998. Signal transduction in the *Caenorhabditis elegans* nervous system. *Annu. Rev. Neurosci.* **21**:279–308

Brading, A.F., Caldwell, P.C. 1971. The resting membrane potential of the somatic muscle cells of *Ascaris lumbricoides*. *J. Physiol.* **217**:605–624

Butler, A., Tsunoda, S., McCobb, D.P., Wei, A., Salkoff, L. 1993. mSlo, a complex mouse gene encoding "Maxi" calcium-activated potassium channels. *Science* **261**:221–224

Chalfie, M., Tu, Y., Euskirchen, G., Ward, W.W., Prasher, D.C. 1994. Green fluorescent protein as a marker for gene expression. *Science* **263**:802–805

Christensen, M., Estevez, A., Yin, X., Fox, R., Morrison, R., McDonnell, M., Gleason, C., Miller III, D.M., Strange, K. 2002. A primary culture system for functional analysis of *C. elegans* neurons and muscle cells. *Neuron* **33**:503–514

Coburn, C.M., Bargmann, C.I. 1996. A putative cyclic nucleotide-gated channel is required for sensory development and function in *C. elegans*. *Neuron* **17**:695–706

Colbert, H.A., Smith, T.L., Bargmann, C.I. 1997. OSM-9, a novel protein with structural similarity to channels, is required for olfaction, mechanosensation, and olfactory adaptation in *Caenorhabditis elegans*. *J. Neurosci.* **17**:8259–8269

Davis, R.E., Stretton, A.O.W. 1989a. Passive membrane properties of motorneurons and their role in long-distance signaling in the nematode *Ascaris*. *J. Neurosci.* **9**:403–414

Davis, R.E., Stretton, A.O.W. 1989b. Signaling properties of *Ascaris* motorneurons: graded active responses, graded synaptic transmission, and tonic transmitter release. *J. Neurosci.* **9**:415–425

del Castillo, J., Morales, T. 1967. The electrical and mechanical activity of the esophageal cell of *Ascaris lumbricoides*. *J. Gen. Physiol.* **50**:603–630

Goodman, M.B., Hall, D.H., Avery, L., Lockery, S.R. 1998. Active currents regulate sensitivity and dynamic range in *C. elegans* neurons. *Neuron* **20**:763–772

Harris, J.E., Crofton, H.D. 1957. Structure and function in the nematodes: Internal pressure and cuticular structure in *Ascaris*. *J. Exp. Biol.* **34**:116–130

Hobson, A.D., Stephenson, W., Beadle, L.C. 1952a. Studies on the physiology of *Ascaris lumbricoides*. I. The relation of the total osmotic pressure, conductivity and chloride content of the body fluid to that of the external environment. *J. Exp. Biol.* **29**:1–21

Hobson, A.D., Stephenson, W., Eden, A. 1952b. Studies on the physiology of *Ascaris lumbricoides*. II. The inorganic composition of the body fluid in relation to that of the environment. *J. Exp. Biol* **29**:22–29

Komatsu, H., Mori, I., Rhee, J.-S., Akaike, N., Ohshima, Y. 1996. Mutations in a cyclic nucleotide-gated channel lead to abnormal thermosensation and chemosensation in *C. elegans*. *Neuron* **17**:707–718

Komatsu, H., Jin, Y.-H., L'Etoile, N., Mori, I., Bargmann, C.I., Akaike, N., Ohshima, Y. 1999. Functional reconstitution of a heteromeric cyclic nucleotide-gated channel of *Caenorhabditis elegans* in cultured cells. *Brain Research* **821**:160–168

Lockery, S.R., Goodman M.B. 1998. Tight-seal whole-cell patch clamping of *Caenorhabditis elegans* neurons. *Meth. Enzymol.* **293**:201–217

Nehrke, K., Begenisich, T., Pilato, J., Melvin, J.E. 2000. Model organisms: new insights into ion channel and transporter function. *Caenorhabditis elegans* ClC-type chloride channels: novel variants and functional expression. *Am. J. Physiol.* **279**:C2052–C2066

Pax, R.A., Geary, T.G., Bennett, J.L., Thompson, D.P. 1995. *Ascaris suum:* Characterization of transmural and hypodermal potentials. *Exp. Parasitol.* **80:**85–97

Richmond, J.E., Jorgensen, E.M. 1999. One GABA and two acetylcholine receptors function at the *C. elegans* neuromuscular junction. *Nat. Neurosci.* **2**:791–797

Robertson, A.P., Martin, R.J. 1996. Effects of pH on a high conductance Ca-dependent chloride channel: a patch-clamp study in *Ascaris suum*. *Parasitology* **113**:191–198

Schriever, A.M., Friedrich, T., Pusch, M., Jentsch, T.J. 1999. CLC chloride channels in *Caenorhabditis elegans*. *J. Biol. Chem.* **274**:34238–34244

Sengupta, P., Chou, J.H., Bargmann, C.I. 1996. *odr-10* encodes a seven transmembrane domain olfactory receptor required for responses to the odorant diacetyl. *Cell* **84**:899–909

Troemel, E.R., Kimmel, B.E., Bargmann, C.I. 1997. Reprogramming chemotaxis responses: sensory neurons define olfactory preferences in *C. elegans*. *Cell* **91**:161–169

Ward, S., Thompson, N., White, J.G., Brenner, S. 1975. Electron microscopical reconstruction of the anterior sensory anatomy of the nematode *Caenorhabditis elegans*. *J. Comp. Neurol.* **160**:313–337

Ware, R.W., Clark, D., Crossland, K., Russell, R.L. 1975. The nerve ring of *Caenorhabditis elegans:* sensory input and motor output. *J. Comp. Neurol.* **162**:71–110

Wei, A., Jegla, T., Salkoff, L. 1996. Eight potassium channel families revealed by the *C. elegans* genome project. *Neuropharmacol.* **35**:805–829

Yuan, A., Dourado, M., Butler, A., Walton, N., Wei, A., Salkoff, L. 2000. SLO-2, a $K^+$ channel with an unusual $Cl^-$ dependence. *Nat. Neurosci* **3**:771–779